Particle Scattering Factor of Pearl Necklace Chains

Ralf Schweins,[1,2] *Klaus Huber**[1]

[1]Universität Paderborn, Fakultät für Naturwissenschaften, Department Chemie, Warburger Str.100, D-33098 Paderborn, Germany
E-mail: huber@chemie.uni-paderborn.de
[2]Institut Laue - Langevin, Large Scale Structures Group, B. P. 156, 6, rue Jules Horowitz, F-38042 Grenoble CEDEX 9, France

Summary: The particle scattering behaviour of a pearl necklace chain is derived. The chain is composed of sphere-like pearls, separated by rod-like segments of fixed length, which have no angular restrictions. By calculating several series of model scattering curves, the important structural features are retrieved. The model is believed to be useful in interpreting intermediate structures of collapsing macromolecules or polyelectrolytes. A first application to a shrinking polyelectrolyte coil generated by molecular dynamic simulations (Limbach and Holm, J.Phys.Chem. 2003) is presented and used to discuss the potentials and limits of the model.

Keywords: coil collapse; form factor; freely jointed chain; pearl necklace; polyelectrolyte collapse

Introduction

Polyelectrolytes are highly charged and water soluble macromolecules. Discharging the polyelectrolytes reduces their solubility. If water is a non-solvent to the respective neutral polymer backbone, electrical discharge eventually leads to a precipitation of a polyelectrolyte salt. This neutralisation of the chains can be caused by protonation, by complexation of metal cations[1-3] or by addition of a large amount of an inert salt.[3-5] Very low concentrations of the polyelectrolyte chains may prevent a macroscopic phase separation for kinetic reasons resulting in an intramolecular collapse to sphere like particles. Predicted by various theoretical approaches, this collapse was established experimentally for the first time with sodium polyacrylate chains (NaPA) in the presence of calcium ions.[6,7]

 DOI: 10.1002/masy.200450702

A similar coil collapse occurs with neutral polymers when crossing the unperturbed or Θ-state.[8-13] First time resolved experiments by means of dynamic light scattering on the collapse mechanism of neutral polymers revealed a two stage kinetics with a crumpled globule in a first stage and a final collapse to a compact globule or sphere. The collapse was inferred by quenching polymer solutions from the Θ-temperature to just below its separation threshold. The time regime for the induced collapse was in the order of a few minutes and required extremely skillful experiments.[12]

Much less experimental data exist on the shrinking mechanism of polyelectrolyte coils close to a phase boundary. In the latter case, however, theoretical progress is remarkable. Consideration of the polyelectrolyte collapse began with the publications by Khokhlov,[14] Kantor and Kardar[15,16] and Rubinstein et al.[17] The underlying physics is the shape instability of charged droplets which depends on the surface tension and charge density. However, unlike to charged droplets, a collapsed chain cannot fall apart. Its conformational transformation from spherically collapsed particles to extended polyelectrolyte coils or vice versa passes a cascade of transition states. Depending on the conditions, these states may adopt cigar like or pearl necklace like structures.[15-22] The transformation can be induced by addition of an increasing amount of an inert salt to a polyelectrolyte, dissolved in a medium which is a bad solvent for its neutral backbone.

First experimental indications for pearl necklace like intermediates adopted by polyelectrolyte chains in dilute solution were published only recently. Geissler et al.[23] induced the shrinking of a polycation in saltless water by addition of acetone and performed small angle neutron scattering (SANS) experiments with collapsed chains. By comparing the overall size of the polycations with the behavior of the scattering curves at high q-values, they found indication for a string of three to four pearls. Similar to this type of shrinking, Morawetz et al.[24] followed solutions of sodium polystyrene-sulfonate, sodium polyacrylate (NaPA) and sodium polymethacrylate (NaPMA) close to the phase boundary by adding methanol to the aqueous solutions and performed NMR spectroscopy. They found a reduction of the ^1H signals which was attributed to the loss of mobile segments. According to Morawetz et al.[24], those segments were used up to form the pearls. The most recent paper in this field[25] also seems to provide the most direct indications. Minko et al. succeeded to produce AFM images which indicate a cascade of structural transitions of poly(2-vinylpyridine) in solution, induced by Pd^{2+} complexation. The cascade started with wormlike chains and finally led to pearl necklace

like structures. At the same time first systematic small angle scattering has been carried out on highly dilute solutions of NaPA in the presence of earth alkaline cations.[26,27] These make the development of theoretical scattering curves for pearl necklace like structures highly desirable.

First theoretical scattering curves[20-22] stem from computer simulations of the collapse process of polyelectrolyte chains induced by counterion condensation. A characteristic feature of those curves is a shoulder or a maximum of the scattering curve at a distinct value of the scattering vector. This value was related to the distance between neighbored pearls.

Initial attempts to calculate analytical scattering curves have been made by Rubinstein et al.[17] and by Francois et al.[28] In Ref. 17, pearls were lined up along a rodlike string. In Ref. 28, the pearls were assumed to be connected by Gaussian chain segments which are modeled by bonds with a Gaussian length distribution without angular correlations. The two models limit the range of flexibility reaching from a rod like arrangement of pearls to a flexible chain of pearls. In both cases, the scattering from strings was neglected which may be justified in the light of the much larger mass fractions being located in the pearls. However, it may become an increasingly crude approximation if the interconnecting strings are coiled segments.

We therefore extend these calculations by a model which is characterized by features. (1) We connect rods of constant length denoted as strings to form a freely jointed chain with pearls on its junctions. (2) We explicitly include the scattering contribution from the interconnecting strings. An appropriate assessment of both features seems to be desirable and is presented in the following. Aside from the explicit consideration of the interconnecting strings, the present model differs from the suggestion by Rubinstein et al.[17] in its angular flexibility. However, we have to emphasize, that the adoption of a certain extent of angular flexibility seems to be realistic only as long as two next but one pearls do not get closer than the length of a string in accord with the Rayleigh instability. A certain extent of angular flexibility may also become a realistic feature for pearl necklace structures which have causes[29] different from the Rayleigh instability of polyelectrolytes. At the same time, our model fixes the string length. This may be a more realistic feature than the distribution width of an interconnecting Gaussian coil segment in the model of Francois et al.,[28] at least if the separation of charged pearls along a polyelectrolyte chain is addressed. Thus, the present model accounts for aspects not

considered by the previous calculations[17,28] without being necessarily superior in all respects. However, it is the application of the different models which may help to distinguish the consequences of various features on the scattering of intermediates of a collapsing polymer.

In the first part of the paper, we describe the model used for the pearl necklace and derive its particle scattering factor. In the second part, an outline is given for the major aspects of the scattering behavior by discussing the impact of systematically varied parameters. Finally, the model is compared with well defined structures Limbach and Holm[22] have generated by means of molecular dynamics simulations.

Calculation of Particle Scattering Factor

The Model. The pearl necklace chain is composed of two elements: Rod like strings are interconnected at their ends to form a freely jointed chain. Each linking point is at the center of a homogeneous sphere corresponding to a pearl. M rod like strings connect M + 1 = N pearls. The overall contour length of the chain is

$$L = M \cdot A \tag{1}$$

with A the fixed distance between centers of two neighboring pearls. No angular correlations exist between any two connected rod like strings. The radius of the pearls is R which reduces the physical length of the strings to l

$$l = A - 2R \tag{2}$$

A detailed illustration of the model is given in Figure 1.

The model can be mapped to any chemically specified macromolecular chain according to

$$m_r = l / b \tag{3a}$$

$$m_s = 4\pi R^3 / 3v_o \tag{3b}$$

which relates the number of monomers in a rod like segment m_r to the length b of the chemical monomer and the number of monomers in a pearl m_s to the monomer volume v_o respectively. The total mass M_w of the polymer chain thus amounts to

$$M_w = M \cdot m_r + N \cdot m_s \tag{4}$$

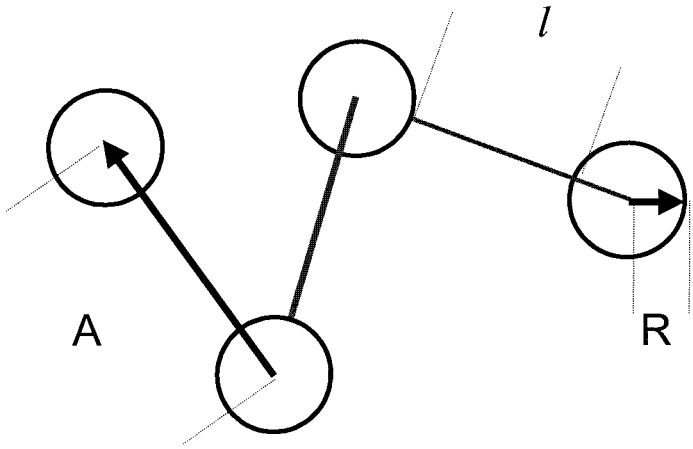

Figure 1. A pearl necklace based on a freely jointed chain with A the distance between the centers of two neighboring pearls, *l* the nearest distance between the surfaces of two neighboring pearls and R the a radius of a pearl.

Elementary Scattering Functions. Independent of the nature of the applied waves, the scattering pattern exerted by a scattering particle can be expressed by the form factor P(q)

$$P(q) = I(q)/I(q = 0) \tag{5}$$

The form factor corresponds to the scattering intensity I(q) as a function of the scattering vector q, normalized by the scattering intensity in forward direction I(q = 0). The scattering vector q is defined as

$$q = (4\pi/\lambda)\sin(\theta/2) \tag{6}$$

with θ the scattering angle and λ the wavelength of the scattered waves.

A suitable starting point for the calculation of particle scattering factors was published in 1915, when Debye first predicted the scattering behavior of small molecules.[30] At that time corresponding scattering curves were about to become accessible by X-ray diffraction. Treating molecules as clusters of atoms with fixed inter-atomic distances r_{ij} , Debye expressed the form factor as a double sum over all atomic pair combinations

$$P(q) = \frac{1}{n^2}\sum_{i=1}^{n}\sum_{j=1}^{n}\psi_i(q)\psi_j(q)\frac{\sin(qr_{ij})}{qr_{ij}} \qquad (7)$$

In Equation (7) the factor $\psi_i(q)$ is the normalized scattering amplitude of the atom i.

In 1969 this formula was used to calculate the form factor of n spheres, lined up on a freely jointed chain. Although, Burchard's and Kajiwara's[31] original intention was to describe the scattering behavior of macromolecules, their results turn out to be an important element for the calculation of the scattering behavior of a pearl necklace. In their model, the spheres corresponded to monomeric units which were connected via bonds of constant length. The bonds fixed the distance between neighboring monomers and formed the freely jointed chain. All monomers were considered to be identical and their scattering behavior could be described by a single normalized scattering amplitude $\psi_i(q) = \psi(q)$. Due to the fact that a sphere is invariant to orientations, the form factor of a sphere is equal to the product $\psi(q)\psi(q)$. Scattering contribution from the bonds were neglected. The resulting scattering curve corresponded to a modified Equation (7)

$$P(q) = \frac{1}{n^2}\psi^2(q)\sum_{i=1}^{n}\sum_{j=1}^{n}\left\langle\frac{\sin(qr_{ij})}{qr_{ij}}\right\rangle \qquad (8)$$

In Equation (8) n is the degree of polymerization of the chain. The brackets < > denote an averaging of the interference factor from two point scatterers, j and i, over all possible conformations of the connecting chain segment with |j-i| monomers. For freely jointed chain segments, this conformational average reads[33]

$$\left\langle \frac{\sin(qr_{ij})}{qr_{ij}} \right\rangle = \left(\frac{\sin qb}{qb} \right)^{|j-i|} \tag{9}$$

In Equation (9) b is the distance between neighboring monomers, corresponding to the bond. By inserting Equation(9) into Equation (8) and solving the double sum, Burchard and Kajiwara reached at

$$P(q) = \frac{2\psi^2(q)}{n^2}\left[\frac{n}{1-\sin(qb)/qb} - \frac{n}{2} - \frac{1-(\sin(qb)/qb)^n}{(1-\sin(qb)/qb)^2} \cdot \frac{\sin(qb)}{qb} \right] \tag{10}$$

A second basic element required for the form factor of a pearl necklace can be recovered from a paper by Hermans and Hermans.[32] Like Burchard and Kajiwara,[31] Hermans' and Hermans' intention was to model the scattering curve of polymeric chains. However, in their case, the monomers were the infinitely thin rods or bonds which form the freely jointed chain. Due to the fact that no angular correlation does exist between two neighboring monomeric bonds, the orientational averaging of each bond was performed independently of the rest of the chain. Starting point is again Equation (8). The scattering behavior of the monomers was expressed by the normalized scattering amplitude of an infinitely thin rod as $\psi_i(q) = \Lambda(q)$. The amplitude $\Lambda(q)$ is an orientational average. Hermans and Hermans could also apply Equation (9) to account for the averaging over all possible distances between monomer i and j. In line with the nomenclature of Equation (8) to Equation (10), we use a chain with m = n-1 bonds each of constant length b. It has to be emphasized that, unlike for spheres, the form factor of a rod is not equal to $\Lambda^2(q)$. The final form of the particle scattering function was[32]

$$P(q) = \frac{\Lambda^2(q)}{m^2}\left[m\left\{ 2/\Lambda(q) - \left(\frac{\sin(qb/2)}{\Lambda(q)qb/2} \right)^2 \right\} + \frac{2m}{1-\sin(qb)/qb} - 2\frac{1-(\sin(qb)/qb)^m}{(1-\sin(qb)/qb)^2} \right] \tag{11}$$

Form Factor of a Pearl Necklace Chain. The particle scattering function of a pearl necklace presented in this paper is based on the freely jointed chain which determines the distances between any two pearls, each located on the ankle of two neighboring bonds (strings). The

scattering curve P(q) decomposes into three contributions. Two of these contributions can be adopted from the elements presented in the preceding section. The term $S_{ss}(q)$ corresponds to the interferences stemming from the pearls and $S_{rr}(q)$ quantifies the interferences of the interconnecting rod like strings. The third contribution $S_{rs}(q)$ is a mixed term, accounting for correlations between the interconnecting strings and the pearls which, to the best of our knowledge, is evaluated for the first time in the present work. Addition of all three contributions and appropriate normalization leads to the form factor of a pearl necklace P(q)

$$P(q) = \frac{S_{ss}(q) + S_{rr}(q) + S_{rs}(q)}{(M \cdot m_r + N \cdot m_s)^2} \tag{12}$$

Normalization is achieved by the total number of chemical monomeric units forming the polymer chain.

The term $S_{ss}(q)$ can be translated from Equation (10) by simply renaming b to A and n to N and by weighting with the amount of monomers $(m_s N)^2$.

$$S_{ss}(q) = 2m_s^2 \psi^2(q)\left[\frac{N}{1-\sin(qA)/qA} - \frac{N}{2} - \frac{1-(\sin(qA)/qA)^N}{(1-\sin(qA)/qA)^2} \cdot \frac{\sin(qA)}{qA}\right] \tag{13}$$

The normalized scattering amplitude for a pearl will be based on a sphere according to[34]

$$\psi(q) = \left[3 \cdot \frac{\sin(qR) - (qR) \cdot \cos(qR)}{(qR)^3}\right] \tag{14}$$

Using the correspondence of m and M, Equation (11) leads to the contribution from the rod like segments to the scattering of a pearl necklace. Here the weighting factor is based on the amount of monomers in all rods $(m_r M)^2$

$$S_{rr}(q) = m_r^2\left[M\left\{2\Lambda(q) - \left(\frac{\sin(ql/2)}{ql/2}\right)^2\right\} + \frac{2M\beta^2(q)}{1-\sin(qA)/qA} - 2\beta^2(q)\frac{1-(\sin(qA)/qA)^M}{(1-\sin(qA)/qA)^2}\right] \tag{15}$$

However, we have to draw attention to an important difference to the Hermans and Hermans model. In the latter case, the scattering of the rod like segments stems from rods with the full length A which is the distance between two neighboring ankles. In the pearl necklace, any connecting rod ends at the surface of two neighboring pearls reducing the effective length to l = A-2R. The remaining parts of A were attributed to the pearls. Thus, two different expressions are required in Equation (15) in order to account for the scattering amplitudes of the rod like segments. The curved bracket is the self term, representing the form factor of an infinitely thin rod of length l. Here $\Lambda(q)$ denotes the orientationally averaged and normalized scattering amplitude of the rod like segments given as[35]

$$\Lambda(q) = \frac{\int_0^{ql} \frac{\sin(t)}{t} dt}{ql} \tag{16}$$

In the remaining two terms of Equation (15), the expression $\beta(q)$ is used to form products of amplitudes corresponding to pair combinations of any two rods which start at R and end at A-R if described in the coordinate system of the preceding pearl respectively

$$\beta(q) = \frac{\int_{qR}^{q(A-R)} \frac{\sin(t)}{t} dt}{ql} \tag{17}$$

Finally, the mixed term remains to be evaluated. This term includes only a part of the double sum in Equation (7). In this part, the index i and j denotes pearls and rod like strings respectively. The scattering amplitude $\psi_i(q) = \psi(q)$ of pearl i is given by Equation (14) and the orientationally averaged and normalized scattering amplitude $\psi_j(q) = \beta(q)$ of a rod j is defined by Equation (17). Casting this term into a double sum and using Equation (9) with A instead of b leads to the mixed term

$$S_{rs}(q) = m_r \beta(q) \cdot m_s \psi(q) \cdot 2 \left[\sum_i^N \sum_j^M \left(\frac{\sin(qA)}{qA} \right)^{\alpha_{ij}} \right] \tag{18}$$

Care has to be taken in properly expressing the exponent α_{ij} which reads

$$\alpha_{ij} = |i-j| \qquad j \geq i \tag{19a}$$

$$\alpha_{ij} = |i-j-1| \qquad j < i \tag{19a}$$

It can easily be shown, that the number of pearl-rod combinations separated by k intermediate rods amounts to 2(N-1-k). Thus by using Equation (19), Equation (18) can be rewritten by the following sum

$$S_{rs}(q) = m_r \beta(q) \cdot m_s \psi(q) \cdot 2\left[2\sum_{k=0}^{N-2}(N-1-k)\left(\frac{\sin(qA)}{qA}\right)^k\right] \tag{20}$$

The sum in Equation (20) can be solved, leading to

$$S_{rs}(q) = m_r \beta(q) \cdot m_s \psi(q) \cdot 4\left[\frac{N-1}{1-\sin(qA)/qA} - \frac{1-(\sin(qA)/qA)^{N-1}}{(1-\sin(qA)/qA)^2} \cdot \frac{\sin(qA)}{qA}\right] \tag{21}$$

Inserting Equation (13), (15) and (21) into Equation (12) finally leads to the form factor of a pearl necklace based on a freely jointed chain.

Parameters. Sodium polyacrylate was chosen as an example for a polyelectrolyte system which is able to collapse to spheres via non-spherical intermediate states.[7,26] A pearl necklace model can be adapted to this system by using a monomer length of b = 2.591 Å and a monomeric volume of v_o = 586.2 Å^3. The latter was estimated from the hydrodynamically effective radius R_h = 170 Å of a completely collapsed sodium polyacrylate chain with a molar mass of $3.3 \cdot 10^6$ Dalton[26,36].

Results

In order to estimate the impact of different structural elements of a pearl necklace on its particle scattering factor, three series of scattering curves were generated.

The first series addresses to the influence of the distance between neighboring pearls at a constant pearl size of R = 80 Å. The distance was varied between 335 Å < A < 510 Å. Results are summarized in Figure 2. All curves exhibit a minimum. The scattering vector of the minimum q_{min} decreases with increasing distance between the neighboring pearls A. In order to estimate a pearl distance A, use can be made from the following empirical relationship

$$A = 10.67 \cdot q_{min}^{-0.83} \qquad (22)$$

A second minimum does not become noticeable due to the lack of correlation between pearls separated by two strings. Above q = 0.03 $Å^{-1}$, all three curves merge and the scattering is governed solely by the individual pearls.

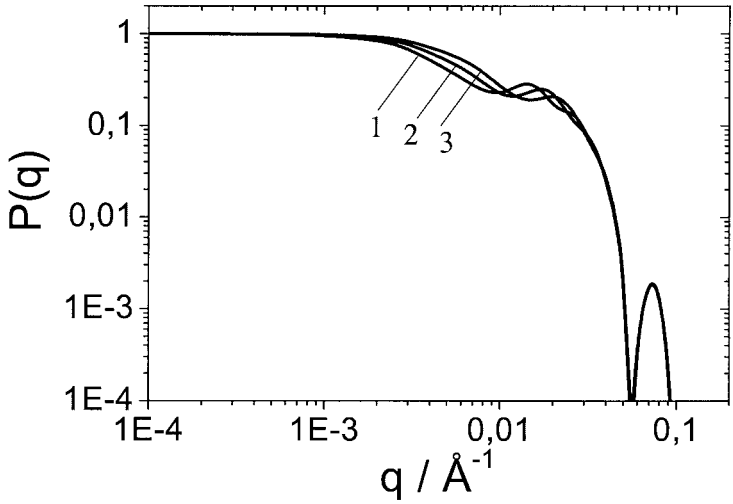

Figure 2. Form factors of pearl necklace chains with three pearls. The pearl size is fixed at R = 80 Å. The distance between two pearls is A = 510 Å (1); A = 410 Å (2) and A = 335 Å (3).

As shown in Figure 3, Equation (22) is reliable in a regime of A/R which is at least as large as 3 < A/R < 6 .

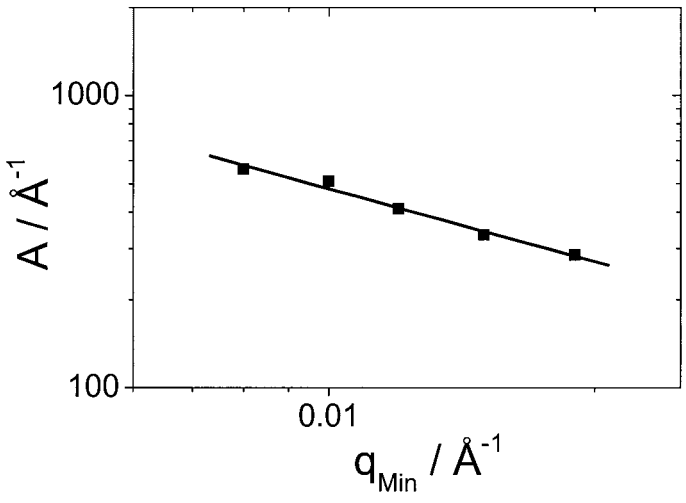

Figure 3. The distance A between the center of two neighboring pearls plotted versus the location of the minimum observed for model scattering curves of trimpbells. The pearl size was fixed at R = 80 Å. The straight line is a fit with Equation (22).

In a second series, the pearl distance is fixed at A = 500 Å and scattering curves are calculated for a variable pearl size in a range of 75 Å < R < 200 Å. Now, the location of the minimum q_{min} remains unchanged at least within this series, but the minimum is getting blurred with increasing R/A and eventually turns into a shoulder. In the case of a shoulder, A could only be estimated by Equation (22) if the inflection point is used instead of q_{min}. However, as shown in Figure 4, another distinct feature becomes discernible. The sharp minimum at q_s moves towards higher q-values for a decreasing pearl size. This could be captured by the empirical equation,

$$R = 4.4 / q_s \qquad (23)$$

which is almost identical to the well known relation $R = 3\pi/2q_s$ for spheres.[34] Clearly, q_s can be attributed to the sphere radius R. Alternatively, the respective maxima to the right of q_s could have equally well been chosen to determine R.

Finally, a series of scattering curves was calculated for variable scattering power of the pearl and rod. This variation was achieved by changing b and v_o , which, according to Equation(3),

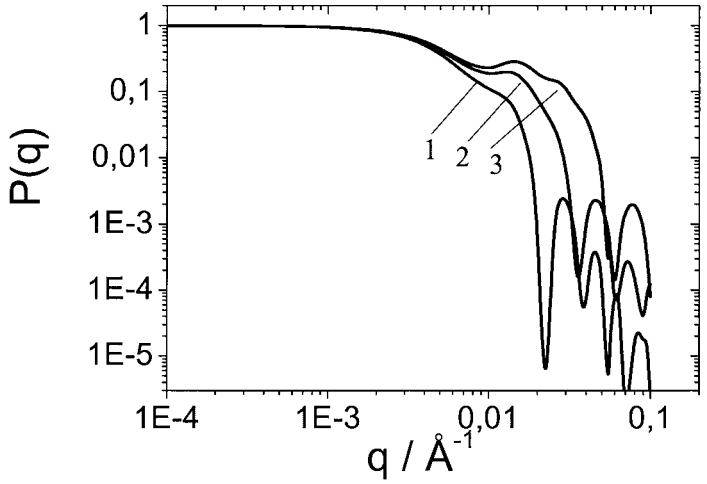

Figure 4. Form factors of pearl necklace chains with three pearls. The distance between neighboring pearls is fixed at A = 500 Å. The pearl size is R = 200 Å (1); R = 125 Å (2) and R = 75 Å (3).

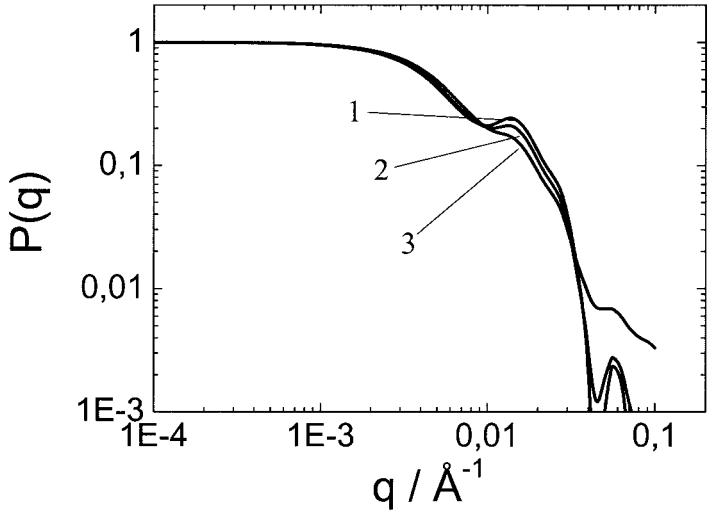

Figure 5. Form factors of pearl necklace chains with three pearls at variable b and v_o. The pearl size and the distance between two neighboring pearls is fixed at R = 100 Å and A = 500 Å respectively. The variation of b and v_o changes the ratio of monomers in a pearl m_s to the number of monomers in an interconnecting rod m_r according to $m_s / m_r = 7146/116$ (1); $m_s / m_r = 6500/1083$ (2) and $m_s / m_r = 5416/2708$ (3).

simply varies the number of monomers per rod m_r and per pearl m_s. In order to isolate this aspect, calculation of the series was performed at a constant distance A between two neighboring pearls and at constant pearl size R. Results are represented in Figure 5. In agreement with the earlier series, the location of the first minimum q_{min} is not affected by the present changes. But the first minimum, which is related to A is smeared out as the ratio m_r/m_s increases and so does q_s.

To conclude, the most prominent feature of our model scattering curves is the minimum q_{min} referring to the distance A between two neighboring pearls. Although q_{min} may not be related to A in a unique way we will demonstrate in the following section, that Equation (22) gives a good enough estimate of A.

Comparison with Simulations by Limbach and Holm

Limbach and Holm[22] performed molecular dynamics simulations with polyelectrolytes at variable solvent quality, strength of electrostatic interaction and charge fraction of the polyelectrolytes. Variation of these properties changes the extent of counterion condensation and thus, the effective charge density of the fully dissociated polyelectrolyte chains. The effective charge of the chains, in turn, determines the size and shape adopted by the chains. Although simulations were performed at a poor solvent quality for the chain backbone, necklace like shapes for the shrinking chains could only be observed in a narrow regime of charge fraction and of strength of electrostatic interaction.

Scattering curves of those intermediates are suitable for a comparison with our model. Their validity lies in the exact knowledge of the corresponding number of pearls, mean pearl size and distance between two neighboring pearls, which are summarized in Table 1. Two intermediate structures were selected: One with an ensemble average number of 1.87 pearls per polyelectrolyte chain and one with an ensemble average number of 2.9 pearls per polyelectrolyte chain. Scattering curves of both selected intermediates were represented in Figure 25 of Ref. 22. The selected curves were compared with scattering curves from our pearl necklace model. Translation of the simulations to an actual length scale in our model was performed by setting $b = 2.591\ Å^{-1} = \sigma$ with σ the unit length used in Ref. 22.

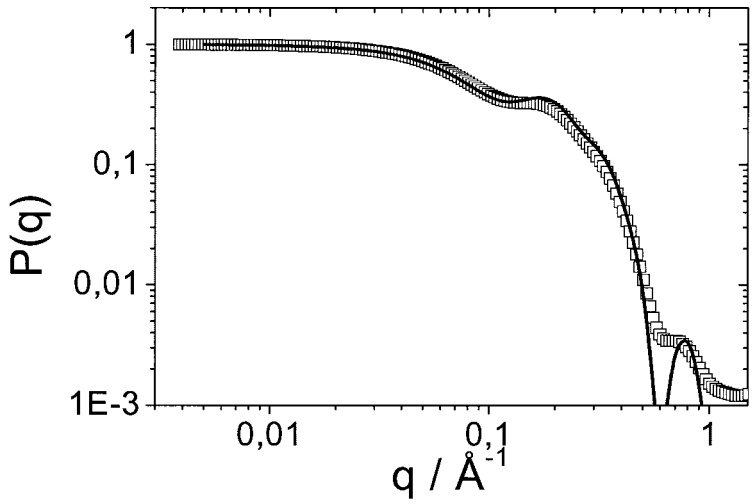

Figure 6. Form factor of an intermediate structure with an ensemble average number of 1.87 pearls per polyelectrolyte chain, generated by molecular dynamics simulations[22] (□) in comparison with the form factor of a dumbbell (—) calculated by Equation (12) with A=40 Å and R=7.5 Å . Parameters are summarized in Table 1.

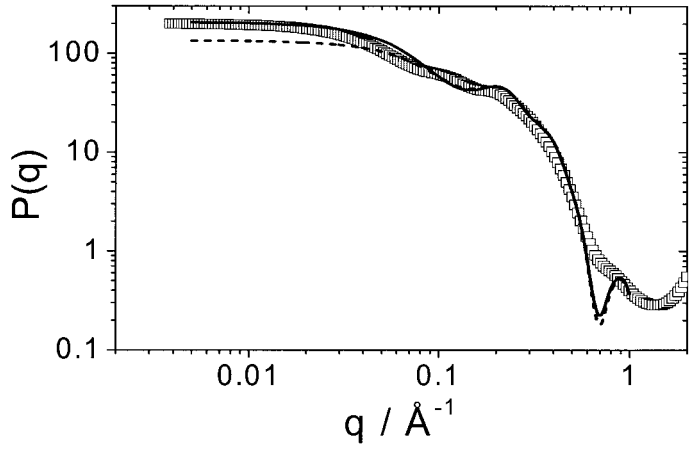

Figure 7. Scattering curve of an intermediate structure with an ensemble average number of 2.9 pearls per polyelectrolyte chain, generated by molecular dynamics simulations[22] (□) in comparison with model scattering curves calculated by Equation (12): Trimpbell (—) with A=35 Å and R=6.5 Å; (---) dumbbell with A=35 Å and R=6.5 Å. All curves are unnormalized and approach M_w in the limit of q=0. Parameters are summarized in Table 1.

With both curves taken from Ref. 22, a value of A and R could be estimated by means of Equation (22) and Equation (23) and compared to the real values known from the simulated samples.[22] As is demonstrated in Table1, agreement is satisfactory. By inserting these estimates for A and R into Equation (12), model curves were calculated for a dumbbell and a trimpbell (necklace with three pearls).

Complete description of the scattering of the simulated dumbbell could be achieved. Results are shown in Figure 6. In the case of the trimpbell, the model curve is adapted to the simulated curve in a regime of $q > 0.12$ Å^{-1}. This was achieved by using the second inflection point to estimate A according to Equation (22). Satisfactory agreement is observed only for $q > 0.12$ Å^{-1} corresponding to the regime, which is dominated by the element of a dumbbell. Agreement is getting poorer for lower q-values. This can clearly be attributed to the stretched shape of the simulated chain, which causes interference effects between two pearls separated by two strings. Such interferences do not occur in our model, which is based on a freely jointed chain. Details can be taken from Figure 7. The very failure is also responsible for the larger radius of gyration R_g observed for the simulated trimpbell (Table 1).

Table 1: Comparison of pearl necklace parameters from molecular dynamics simulations[22] with the corresponding parameters from the theoretical curves for the present pearl necklace model shown in Figure 6 and 7. The parameters corresponding to the model curves are estimates based on an application of Equation (22) and Equation (23) to the scattering curves from molecular dynamics simulation.

Simulation by Limbach and Holm[22]				**Pearl necklace model**			
n_p	A	R[§]	R_g	n_p	A	R	R_g
	Å	Å	Å		Å	Å	Å
1.87	38.9	8.7	19.1	2	40	7.5	20.4
2.90	36.0	7.1	29.7	3	35	6.5	23.0

[§]Estimated from the average radius of gyration of a pearl devided by 0.78

However, proper estimates of R and A could be extracted even in the case of the trimpbell. We simply took advantage of the fact that a q-regime exists, which is dominated by the element of a dumbbell, irrespective of the size of the pearl necklace. This is illustrated in Figure 7 where unnormalized scattering curves were used. The theoretical curves of a trimpbell and a dumbbell, which have the same pearl size R and pearl distance A are compared. Clearly, the simulated trimpbell and the trimpbell and dumbbell based on the freely jointed chain show the same features if $q > 0.12$ Å^{-1} , i. e. a shoulder/minimum at $q_{min} = 0.15$ Å^{-1} and a shoulder/minimum at $q_s = 0.7$ Å^{-1}.

Conclusions

Particle scattering curves could be derived for pearl necklace chains based on a freely jointed chain. The chains consist of two components, homogeneous spheres and infinitely thin rods. The pearls are connected by the rod like segments which have a constant length. Both components contribute to the scattering of the pearl necklace.

The scattering curves have a characteristic shoulder or minimum. Its location correlates with the distance between neighboring pearls. For scattering vectors larger than this location, the scattering behavior is dominated by the individual pearls.

Model scattering curves were compared with molecular dynamics simulations performed by Limbach and Holm.[22] A successful description of simulated data with model curves was only successful in the case of a dumbbell, which was the most simple case. In the case of a trimpbell, the model could not reproduce correlations which stem from pearls separated by two rods. As already pointed out by Limbach and Holm,[22] simulated pearl necklace intermediates generated from fully dissociated polyelectrolyte chains by simple counter ion condensation are highly stretched entities. For this type of shrinking process, the model of Rubinstein et al.[17] is superior to our freely jointed pearl necklace.

Irrespective of the degree of flexibility of a pearl necklace, the structural element of a dumbbell plays a central role in the proof of a pearl necklace shape. A correlation between neighboring pearls and intra-spherical interferences are the most frequent features in the scattering curve. Once these features become discernible in a scattering experiment, they give access to A and R by simply mapping the appropriate section of the experimental curve to the dumbbell scattering curve.

Acknowledgement. Financial support of the Deutsche Forschungsgemeinschaft, Schwerpunktprogramm "Polyelektrolyte mit definierter Molekülarchitektur" SPP 1009, is gratefully acknowledged. The authors are indebted to H. J. Limbach, Ch. Holm and K. Kremer for making available the data of two scattering curves including helpful comments.

[1] F. T. Wall, J. W. Drenan, *J. Polym. Sci.* **1951**, *7*, 83.
[2] I. Michaeli, *J. Polym. Sci.* **1960**, *48*, 291.
[3] A. Ikegami, N. Imai, *J. Polym. Sci.* **1962**, *56*, 133.
[4] H. Eisenberg, G. R. Mohan, *J. Phys. Chem.* **1959**, *63*, 671.
[5] H. Eisenberg, E. F. Casassa, *J. Polym. Sci.* **1960**, *47*, 29.
[6] K.Huber, *J. Phys. Chem.* **1993**, *97*, 9825.
[7] R. Schweins, K. Huber, *Eur. Phys. J. E* **2001**, *5*, 117.
[8] M. Meewes, J. Ricka, M. de Silva, R. Nyffenegger, Th. Binkert, *Macromolecules* **1991**, *24*, 5811 and references therein.
[9] C. Wu, S. Zhou, *Macromolecules* **1995**, *28*, 5388.
[10] C. Wu, S. Zhou, *Macromolecules* **1995**, *28*, 8381.
[11] X. Wang, X. Qiu, C. Wu, *Macromolecules* **1998**, *31*, 2972.
[12] B. Chu, Q. Ying, A. Y. Grosberg, *Macromolecules* **1995**, *28*, 180.
[13] B. Chu, Q. Ying, *Macromolecules* **1996**, *29*, 1824.
[14] A. R. Khokhlov, *J. Phys. A: Math. Gen.* **1980**, *13*, 979.
[15] Y. Kantor, M. Kardar, *Europhys. Lett.* **1994**, *27*, 643.
[16] Y. Kantor, M.Kardar, *Phys. Rev. E* **1995**, *51*, 1299.
[17] A. V. Dobrynin, M. Rubinstein, S. P. Obukhov, *Macromolecules* **1996**, *29*, 2974.
[18] F. J. Solis, M. Olvera de la Cruz, *Macromolecules* **1998**, *31*, 5502.
[19] U. Micka, Ch. Holm, K. Kremer, *Langmuir* **1999**, *15*, 4033.
[20] P. Chodanowski, S. Stoll, *J. Chem. Phys.* **1999**, *111*, 6069.
[21] A. V. Lyulin, B. Dünweg, O. V. Borisov, A. A. Darinskii, *Macromolecules* **1999**, *32*, 3264.
[22] H. J. Limbach, Ch. Holm, *J. Phys. Chem. B* **2003**, accepted.
[23] V. O. Aseyev, S. I. Klenin, H. Tenhu, I. Grillo, E. Geissler, *Macromolecules* **2001**, *34*, 3706.
[24] M.-J. Li, M. M. Green, H. Morawetz, *Macromolecules* **2002**, *35*, 4216.
[25] A. Kiriy, G. Gorodyska, S. Minko, W. Jaeger, P. Štepánek, M. Stamm, *J. Am. Chem. Soc.* **2002**, *124*, 13454.
[26] R. Schweins, P. Lindner, K. Huber, *Macromolecules* **2003**, submitted.
[27] R. Schweins, G. Goerigk, M. Ballauff, K. Huber, in preparation.
[28] C. Heitz, M. Rawiso, J. Francois, *Polymer*, **1999**, *40*, 1637.
[29] Yu. A. Kuznetzov, E. G. Timoshenko, K. A. Dawson, *J. Chem. Phys.* **1995**, *103*, 4807 and *J. Chem. Phys.* **1996**, *104*, 3338.
[30] P. Debye, *Ann. Phys. Leipzig* **1915**, *46*, 809.
[31] W. Burchard, K. Kajiwara, *Proc. Roy. Soc. Lond.* **1970**, *A 316*, 185.
[32] J. Hermans, J. J. Hermans, *J. Phys. Chem.* **1958**, *62*, 1543.
[33] S. Chandrasekhar, *Rev. Mod. Phys.* **1943**, *15*, 1.
[34] Rayleigh, Lord *Proc. Roy. Soc.* **1914**, *A 90*, 219.
[35] T. Neugebauer, *Annalen der Physik* **1943**, *42*, 509.
[36] R. Schweins, K. Huber, *Polymer* **2003**, submitted.